ACS OMEGA

http://pubs.acs.org/journal/acsodf
Article

Experimental Study on NO_x Reduction of Diesel Engine by EGR Coupled with SCR

Published as part of ACS Omega virtual special issue "3D Structures in Medicinal Chemistry and Chemical Biology".

Size Zhang, Xuexuan Nie,* Yuhua Bi, Jie Yan, Shaohua Liu, and Yiyuan Peng

Cite This: ACS Omega 2024, 9, 8308−8319
Read Online
ACCESS | Metrics & More | Article Recommendations

ABSTRACT: Exhaust gas recirculation (EGR) and selective catalytic reduction (SCR) are crucial technologies for mitigating nitrogen oxide (NO_x) emissions in diesel engines. Although EGR reduces engine outlet NO_x emissions, it simultaneously increases diesel consumption, leading to a poor economic performance. SCR requires AdBlue consumption; thus, striking the right balance for overall engine economy is of utmost importance. This study aims to evaluate NO_x emission control and fluid cost in diesel engines. The total fluid cost of the diesel engine includes diesel and AdBlue. The engine is equipped with an aftertreatment system comprising a diesel oxidation catalyst (DOC), diesel particulate filter (DPF), selective catalytic reduction (SCR), and ammonia slip catalyst (ASC). The study was carried out at 1600 and 2100 rpm (25, 50, 75, and 100% load). The results show that with the increase of EGR valve opening, the exhaust temperature increased, the brake-specific fuel consumption (BSFC) increased, and the NO_x emission decreased. With the increased AdBlue dosage, the NO_x conversion efficiency gradually improved, ultimately approaching near-zero NO_x emissions. However, as NO_x emissions decreased, the equivalent diesel fluid cost rose. At 1600 r/min (100% load), when the NO_x emissions were reduced by zero, the maximum fluid costs were 235, 223, and 218g/(kW·h) under the AdBlue/diesel price ratios of 1/1, 1/2, and 1/3, respectively. As the AdBlue/diesel price ratio decreases, the influence of EGR on the fluid cost diminishes. Coordinated control of EGR and AdBlue allows for reduced NO_x emissions while mitigating the overall cost of diesel engines and aftertreatment systems. This research provides valuable guidance for EGR and urea control in diesel engines and contributes to the field of diesel engine emission control.

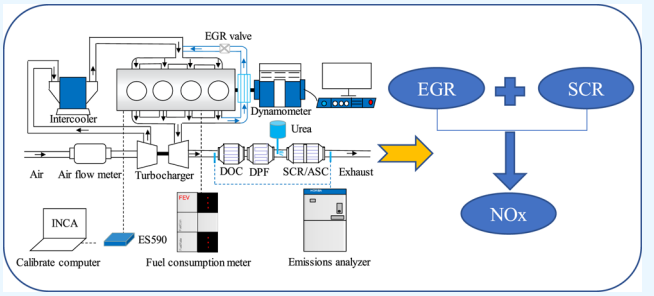

KEYWORDS: *diesel, emission, EGR, SCR, AdBlue, NO_x, temperature*

1. INTRODUCTION

Diesel engine is the main power of road transportation, nonroad mobile machinery, and national defense equipment in the world.[1,2] However, diesel engines produce a large number of pollutants, including HC, CO, NO_x, and PM, which will cause great harm to the environment and human health.[3−6] In order to solve these exhaust pollutants, diesel engine adopts a series of emission control technology, mainly including EGR (for NO_x reduction), DOC (for CO and HC reductions), DPF (for PM reduction), and SCR (for NO_x reduction).[7−9] AdBlue is a urea aqueous solution, also known as diesel exhaust fluid (DEF), which is usually composed of 32.5% urea and 67.5% water. At present, advanced postprocessing technologies mainly include ccSCR (close-coupled selective catalytic reduction)+DOC+DPF+SCR+ASC,[10] electric heating technology,[11] and solid SCR technology,[12] all of which are used to solve low-temperature NO emissions.

Among these pollutants, the most difficult to control is NO_x emissions but also the current diesel engine emission control technical difficulties.[13−15] Many scholars have done a lot of research on NO_x emissions and also proposed a variety of efficient technologies to reduce NO_x emissions. Wang et al.[16] used variable nozzle turbocharging technology VNT and EGR coupling technology to reduce NO_x emissions in a plateau environment. Park et al.[17] proposed a dual-loop exhaust gas recirculation (EGR) system combining the characteristics of high-pressure (HP) and low-pressure (LP) systems to improve diesel engine combustion and NO_x emission performance.

Received: November 14, 2023
Revised: January 23, 2024
Accepted: January 26, 2024
Published: February 8, 2024

https://doi.org/10.1021/acsomega.3c09052
ACS Omega 2024, 9, 8308−8319

Shiyu et al.[18] used a close-coupled selective catalyst reduction (ccSCR) technology to achieve ultralow NO_x emissions. The results show that the NO_x emission of the composite tail pipe was reduced to 0.027 g/(kW·h) under the FTP cycle, which can meet the California Air Resources Board (CARB) ultralow NO_x emission regulations. Zhang et al.[19] used a high-pressure selective catalytic reduction (HP-SCR) system arranged in front of the turbine, which is suitable for high-power marine low-speed engines and can effectively reduce nitrogen oxide emissions. However, the HP-SCR reactor will cause an increase in engine exhaust back pressure, affecting its performance and brake-specific fuel consumption (BSFC). Liu and Tan[12] studied the experimental study of solid SCR technology to reduce NO_x emissions from diesel engines. The results show that based on the same ammonia−nitrogen ratio setting, the World Harmonized Steady Cycle (WHSC) NO_x conversion efficiency is improved by 3.3% and the World Harmonized Transient Cycle (WHTC) NO_x conversion efficiency is increased by 4.5%. Nie et al.[20] studied the effect of exhaust thermal management on NO_x emission. The results showed that NO_x conversion efficiency was improved by intake or exhaust throttling or post injection at any altitudes. Lou et al.[21] studied the effect of EGR combined with SCR on the NO_x emission characteristics of a heavy-duty diesel engine based on the engine bench test. The results showed that the NO reduction rate of EGR-coupled SCR increased with the increase of the engine load, and the effect was no longer significant when the NO reduction rate exceeded a certain limit under the same working conditions.

Although there are many technologies to reduce NO_x emissions, EGR and SCR technologies are the most widely used and mature key technologies to solve NO_x emissions. One is the internal purification technology, and the second is the external post-treatment technology. Domestic and foreign scholars have done a lot of work on EGR and SCR technology research. Ju et al.[22] conducted a related study using GT-POWER one-dimensional simulation software, and the results showed that the use of EGR decreases diesel engine dynamics, economy, and NO_x emissions and delays the moment of ignition and decreases boost pressure under some operating conditions. Mohiuddin et al.[23] investigated the effect law of EGR on diesel engine performance through bench tests, and the results showed that the NO_x and carbon soot trade-off relationship varied more significantly with EGR rate when the compression ratio was higher and was more pronounced at low and medium loads than at high loads. Kumar et al.[24] studied the effect of EGR on diesel engine emission performance by ANSYS 3D simulation software and found that NO_x emission decreases while CO_2 emission increases with increasing EGR rate, so carbon traps were designed to reduce NO_x and CO_2 emissions simultaneously with EGR. Kumar et al.[25] studied the matching of EGR with the post-treatment system experimentally and showed that EGR can be well matched with DPF or SCR respectively at EGR rates of 10−20% and EGR can be well matched with DPF+SCR at the EGR rate of 10%. Cheng et al.[26] studied the effect law of EGR on the performance of low-load diesel engine by bench test and found that as the EGR rate increases, the maximum in-cylinder burst pressure and heat release rate decrease and the average in-cylinder temperature decreases; when the EGR rate is low, the smoke increases with the increase of EGR rate, while with the further increase of the EGR rate, the smoke emission decreases and the CO and HC emissions increase rapidly. Zhang et al.[27] designed a system in which the EGR gas component enters the cylinder simultaneously with oxygen, and the incoming oxygen with EGR can reduce both NO_x and carbon soot emissions from diesel engines.

For the study of urea injection, Mehregan and Moghiman[28] designed an experimental scheme using an orthogonal method to investigate the effect of different urea injection parameters on the SCR conversion efficiency of biodiesel engines, and the results showed that increasing the urea concentration, urea injection volume, and urea injection angle can effectively reduce NO_x emissions, while the orthogonal test design variance indicated that the urea concentration and urea injection volume were the most significantly influential parameters. Diao et al.[29] conducted a study on the performance of diesel SCR urea pumps through bench tests, and the results showed that as the urea injection volume increased, the NO_x conversion efficiency increased and NO_x emissions downstream of SCR decreased significantly, but when the urea injection volume increased to a certain level, it caused a significant increase in ammonia escape. Tan et al.[30] conducted an experimental study of selective catalytic reduction failure at low ammonia-to-nitrogen ratios and their urea injection deficiency test results showed that as the urea injection increased, the ammonia-to-nitrogen ratio increased and the NO_x conversion efficiency rose, but ammonia leakage also increased.

For the study of SCR temperature, Qiu et al.[31] carried out the temperature characteristic test of the inlet and outlet of the SCR system on the bench and arranged the SCR carrier temperature sensor to collect the temperature, which provided data support for the subsequent Matlab/Simulink modeling. Schönebaum et al.[32] studied the effect of the LNT-SCR combined system on ammonia storage and NO_x emissions and the five thermocouples (K-type) in each catalyst to study the temperature distribution of the entire catalyst.

From the above research, it mainly focuses on the influence of EGR on the power, economy, emission, and combustion performance of diesel engine, as well as the influence of key parameters of the urea injection system on the performance of the SCR system. However, there are few studies on the influence of EGR coupling urea injection amount, SCR carrier temperature, and NO_x emissions.

The purpose of this paper is to analyze the NO_x emission capacity and the total cost of the diesel engine under different EGR and AdBlue. The effects of EGR valve opening and AdBlue rate on the engine air flow rate, air−fuel ratio (AFR), exhaust temperature, NO_x emissions, the fuel consumption, SCR carrier temperature, NO_x conversion efficiency, and the total cost of diesel engine were comprehensively studied. By analyzing the effects of different EGR and AdBlue on the engine and SCR, the final coupling was to solve the final NO_x emissions, so as to achieve the best economic performance. This research work can provide guidance for EGR control and urea control of diesel engine.

2. EXPERIMENTAL SETUP AND METHODS

2.1. Testing Equipment. The test engine was a four-cylinder high-pressure common-rail diesel engine equipped with an exhaust gas recirculation (EGR) system. Its main technical parameters are listed in Table 1. The main instruments in the test included an FEV measurement and control system, an FEV dynamometer, an FEV air flow rate meter, an FEV fuel consumption meter, and two Horiba

https://doi.org/10.1021/acsomega.3c09052
ACS Omega 2024, 9, 8308−8319

Table 1. Main Engine Parameters

parameter	value
air system	turbocharged, intercooled
bore × stroke	81 mm × 97 mm
engine displacement	1.99 L
engine compression ratio	16.2:1
peak torque	350 N·m at 1600−2400 r/min
rated power	90 kW at 3200 r/min

emissions analyzer. Figure 1 shows the engine testing layout diagram. Figure 2 shows the test bench diagram. The primary

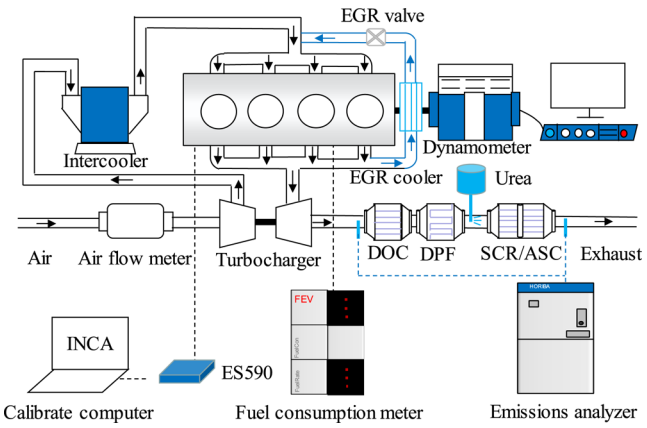

Figure 1. Schematic diagram of the experimental setup.

characteristics of the measurement instruments are listed in Table 2. The engine was equipped with a DOC+DPF+SCR +ASC exhaust aftertreatment system, and the catalyst parameters are shown in Table 3.

2.2. Experiment Method. *2.2.1. Engine Operating Conditions Selected.* 1600 and 2100 r/min (25, 50, 75, and 100% load, the corresponding torque was 350, 262.5, 175, and 87.5 N·m) were used to study the effects of different EGR valve openings and AdBlue rates on NO_x emissions and total fluid cost. The engine brake torque was kept constant at every engine load in this study.

2.2.2. EGR Valve Control and AdBlue Control. EGR valve opening and AdBlue rate are controlled by INCA calibration

Table 2. Measuring Accuracy of Measuring Devices

measuring device	manufacturer/type	variable measured	accuracy
dynamometer	Qdi28.3-2FI	engine speed	<±0.1% full scale
		engine torque	<±0.2% full scale
exhaust gas analyzer	Horiba MEXA-7500DEGR	HC emission	<±1.0% full scale
		CO emission	<±1.0% full scale
		NO_x emission	<±1.0% full scale
fuel consumption meter	FEV fuelcon	fuel consumption	<±0.05% full scale
air flow meter	ABB/50MC2-6F	engine air flow rate	±1.0% measured value
exhaust temperature sensor	KX391A-K-XL	SCR temperature	<±0.5% full scale

software. During the study, the EGR valve opening was increased by 10% from closed to maximum. The AdBlue rate increases from 0 to 20 mg/s successively until the final NO_x emission was zero.

2.2.3. SCR Carrier Temperature Test. Exhaust temperature is an important factor affecting the efficiency of SCR, so the test of SCR carrier temperature was carried out for different schemes to explore the temperature characteristics of the SCR carrier. In this study, we used nine temperature sensors to measure the SCR carrier temperature. Figure 3 shows the whole process of the temperature test and the test positions of nine temperature sensors.

2.2.4. The Methods of Emission Measurement. The sampling tubes of two emission analyzers were placed before and after the postprocessing system for measuring NO_x emissions.

2.3. Baseline Engine Performance. Figure 4 shows the mapping characteristics of engine at 1000−3200 r/min. At the different speed−load modes, the engine air flow rate, the BSFC, the turbine inlet temperature, the SCR inlet temperature, the NO_x emissions, and the AdBlue rate exhibited different trends. These maps serve as a reference for later

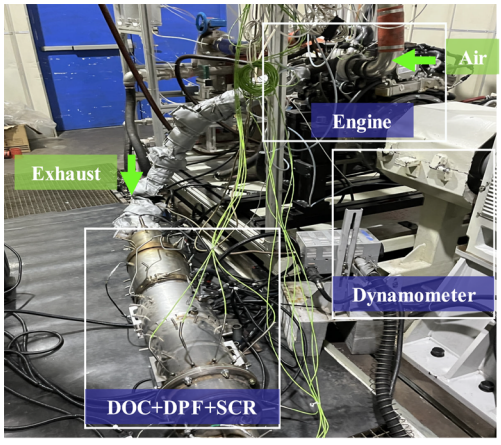

(a) Engine and after-treatment system

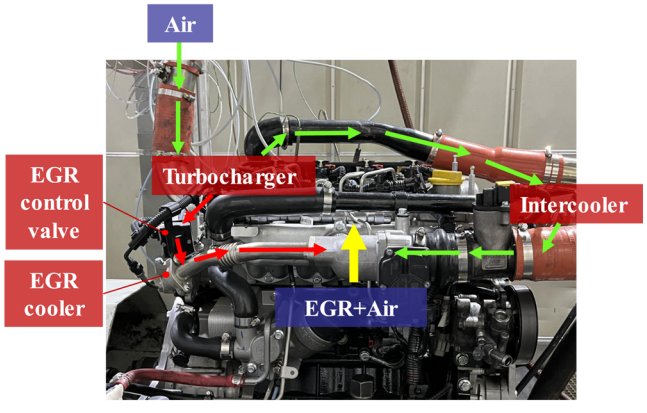

(b) Photographic representation of EGR

Figure 2. Diagram of the test bench. (a) Engine and aftertreatment system. (b) Photographic representation of EGR.

https://doi.org/10.1021/acsomega.3c09052
ACS Omega 2024, 9, 8308−8319

Table 3. Catalyst Parameters

	DOC	DPF	SCR	ASC
carrier material	cordierite	cordierite	cordierite	cordierite
catalyst shape	cylindrical	cylindrical	cylindrical	cylindrical
catalyst size	143 mm (D) × 101 mm (L)	190 mm (D) × 177 mm (L)	190 mm (D) × 101 mm (L)	190 mm (D) × 76 mm (L)
catalyst cell density ($1/in^2$)	400 CPSI	300 CPSI	600 CPSI	600 CPSI

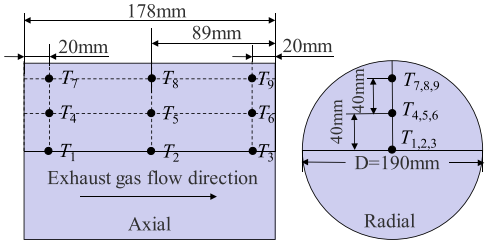

Figure 3. Position of the SCR temperature sensor.

research. The fuel consumption characteristics of the diesel engine are the lowest at 75% load.

3. RESULTS AND DISCUSSION

3.1. Effects of EGR Valve Opening. *3.1.1. Effects of EGR on Engine Air Flow Rate and Air−Fuel Ratio.* Figure 5 shows the impacts of the EGR valve opening on the engine air flow rate and air−fuel ratio (AFR) under different engine loads at 1600 and 2100 r/min. The constant torque method was used in the experiment. Due to the limitation of engine power, the actual maximum of EGR valve opening that can be opened at different speeds was different, resulting in different numbers of data points at 1600 and 2100 speeds. When the EGR valve opening increased, the engine air flow rate and AFR decreased. With the increase of engine speed and load, the demand of engine air flow rate increased and the AFR decreased. After the EGR valve was opened, the exhaust gas acts as part of the fresh air, so the engine air flow rate decreases. In addition, due to the exhaust mass flow increase, the proportion of fresh air decreases, leading to reductions in the AFR. At 1600 r/min, the EGR valve can be opened up to 30%; when the EGR valve opening was increased by every 10%, the engine air flow rate decreases by 14.4, 12.4, 11.1, and 3.5 kg/h respectively under 25, 50, 75, and 100% load, respectively. At 2100 r/min, the EGR valve can be opened up to 30%; when the EGR valve opening was increased by every 10%, the engine air flow rate decreases by 23.8, 15.2, 12.6, and 9.7 kg/h, respectively, under 25, 50, 75, and 100% load.

3.1.2. Effects of EGR on BSFC. Figure 6 shows the impacts of the EGR valve opening on the BSFC under different loads at 1600 and 2100 r/min. As the EGR valve opening was increased, the BSFC increased. It can be seen from the figure that the BSFC was the highest at 25% load, followed by 100, 50, and 75% load. This was determined by the mapping characteristics of engine, and the BSFC was the lowest at medium load. At 1600 r/min, the BSFC increased by 1.0, 0.7, 0.8, and 1.6 g/(kW·h) for each 5% increase in EGR valve opening at 25, 50, 75, and 100% loads, respectively. At 2100 r/min, the BSFC increased by 1.1, 0.7, 0.8, and 1.0 g/(kW·h) for each 5% increase in EGR valve opening at 25, 50, 75, and 100% loads, respectively. These phenomena were because the engine air flow rate reduction caused by the EGR resulted in combustion deterioration. The air−fuel ratio change was the main cause of the BSFC increase when EGR valve opening was increased.

3.1.3. Effects of EGR on NO_x Emission. Figure 7 shows the impacts of the EGR valve opening on the NO_x emissions at the engine outlet under different loads at 1600 and 2100 r/min. As the EGR valve opening was increased, the engine outlet NO_x emissions decreased, because the EGR reduced the combustion temperature in the cylinder. The engine outlet NO_x emissions were the highest at 100% load, followed by 75, 50, and 25% load; this is caused by the high exhaust temperature of the engine at high load. At 1600 rpm, the engine outlet NO_x emissions decreased by 2.2, 2.1, 1.2, and 0.8 g/(kW·h) for each 5% increase in EGR valve opening at 25, 50, 75, and 100% loads, respectively. At 2100 r/min, the engine outlet NO_x emissions decreased by 3.5, 2.0, 1.8, and 1.7 g/(kW·h) for each 5% increase in EGR valve opening at 25, 50, 75, and 100% loads, respectively. As can be seen from the figure, with the increase of engine speed, the EGR valve opening had a greater impact on NO_x emission. Therefore, it shows that the EGR valve opening can be appropriately increased at high speed to reduce the NO_x emission at a high load.

3.1.4. Effects of EGR on Exhaust Temperature. Figure 8 shows the impacts of the EGR valve opening on the exhaust temperature under different loads at 1600 and 2100 r/min. The exhaust temperature refers to the engine outlet temperature, which was the supercharger turbine inlet temperature. As the EGR valve opening was increased, the exhaust temperature increased. It can be seen from the figure that the exhaust temperature was the highest at 100% load, followed by 75, 50, and 25% load. At 100% load of 1600 r/min, the exhaust temperature increases by 10.7 °C for every 5% increase in EGR. The reason for the increase of exhaust temperature was that after the EGR valve was opened, the proportion of fresh air entering the cylinder decreases and the combustion in the cylinder becomes worse, resulting in the prolonged combustion duration and the increase of the exhaust temperature.

3.1.5. Effects of EGR on SCR Carrier Temperature. Figure 9 shows the impacts of the EGR valve opening on the SCR carrier temperature under different loads at 2100 r/min. The SCR carrier temperature was a crucial factor in urea reaction. Exploring the internal temperature of the SCR carrier was helpful for NO_x emission control. After the EGR valve was opened, the intake flow rate of the engine decreases, so does the exhaust mass flow rate. As a result, the exhaust flow velocity of the engine changes, ultimately affecting the temperature of the SCR carrier. Too high or too low temperature of SCR carrier made the catalyst efficiency low.

It can be seen from the figure that the center temperature of the SCR carrier was high and the edge temperature was low, which was caused by uneven airflow. The reasonable design of the mixer was the key to the uniform distribution of the SCR temperature and urea. On the other hand, the front-end temperature of the SCR carrier was lower and the back-end temperature was higher. This was due to the urea attached to the SCR front-end, resulting in the SCR front-end temperature

https://doi.org/10.1021/acsomega.3c09052
ACS Omega 2024, 9, 8308−8319

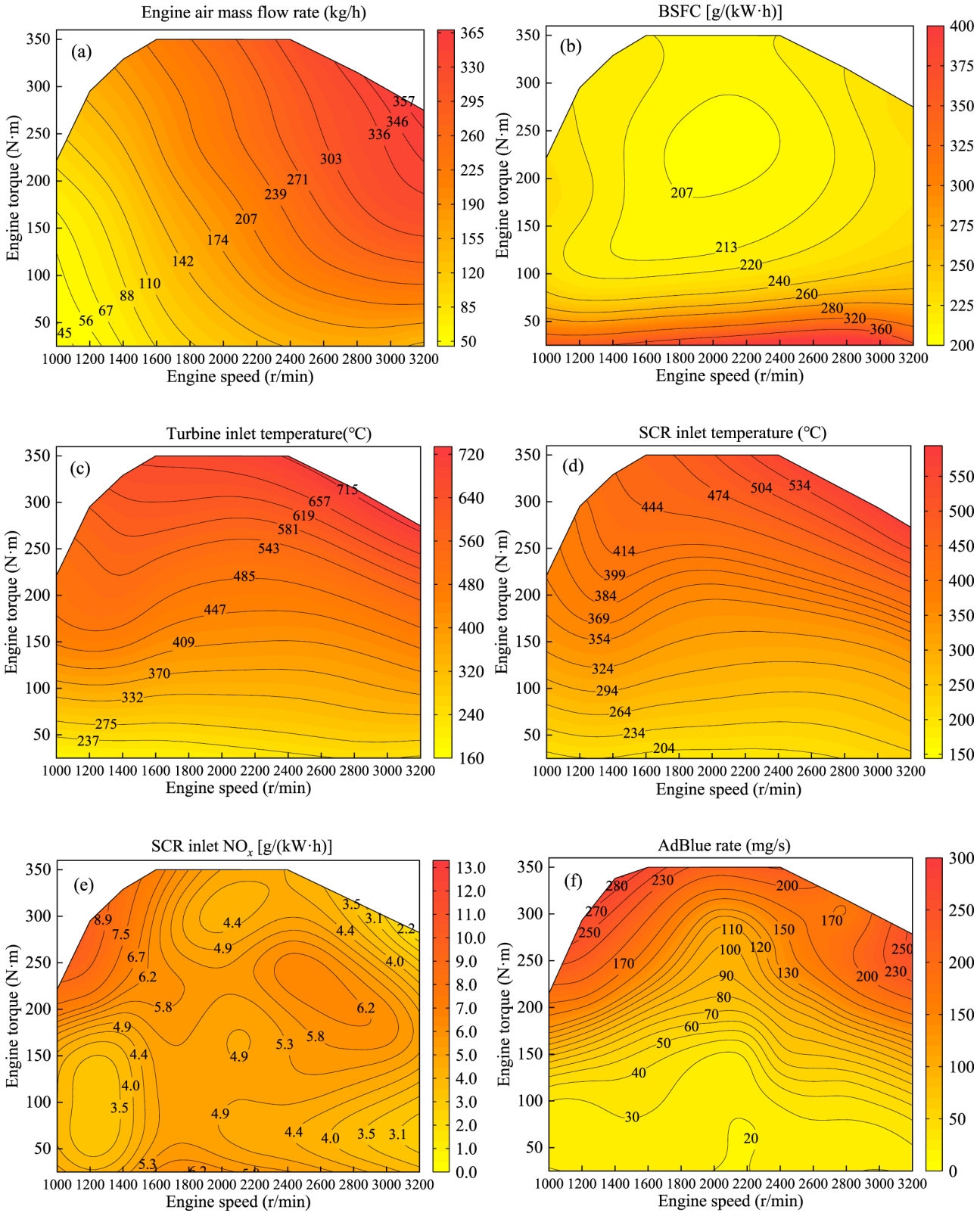

Figure 4. Baseline engine performance under mapping characteristics. (a) Engine air mass flow rate. (b) BSFC. (c) Turbine inlet temperature. (d) SCR inlet temperature. (e) SCR inlet NO_x. (f) AdBlue rate.

being lower than the back-end temperature. At 50% load of 2100 r/min, the mean cross section temperatures of the SCR carrier center were 305.5, 309.1, and 311.2 °C at the EGR valve opening of 14, 20, and 30%, respectively. The average temperatures of the cross section at half radius of the axial direction were 304.2, 308.7, and 311.2 °C, respectively. The average temperatures of the edge cross section were 285.2, 286.7, and 288.6 °C, respectively. At 75% load of 2100 r/min, the mean cross section temperatures of the SCR carrier center were 369.9, 371.8, and 372.7 °C at EGR valve openings of 10,

https://doi.org/10.1021/acsomega.3c09052
ACS Omega 2024, 9, 8308−8319

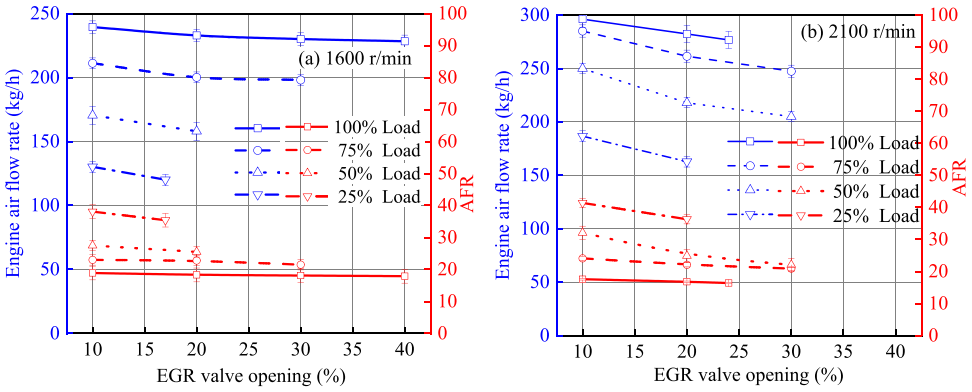

Figure 5. Effects of EGR on engine air flow rate and AFR under different loads: (a) 1600 r/min. (b) 2100 r/min.

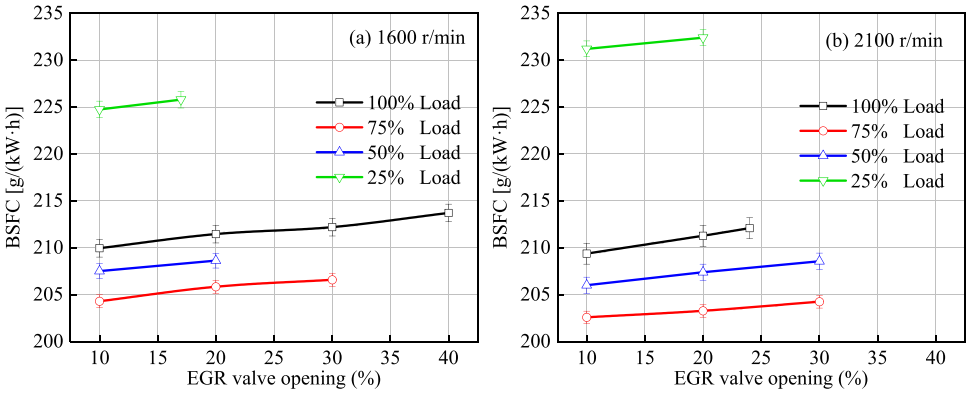

Figure 6. Effects of EGR valve opening on BSFC under different loads: (a) 1600 r/min. (b) 2100 r/min.

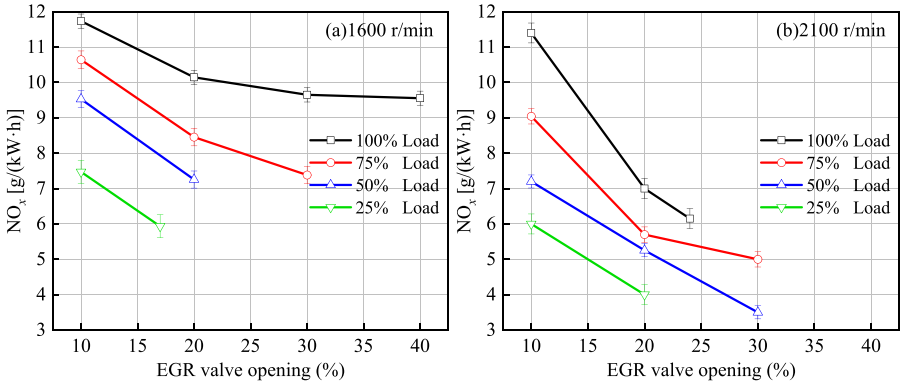

Figure 7. Effects of EGR valve opening on NO_x emission under different loads: (a) 1600 r/min and (b) 2100 r/min.

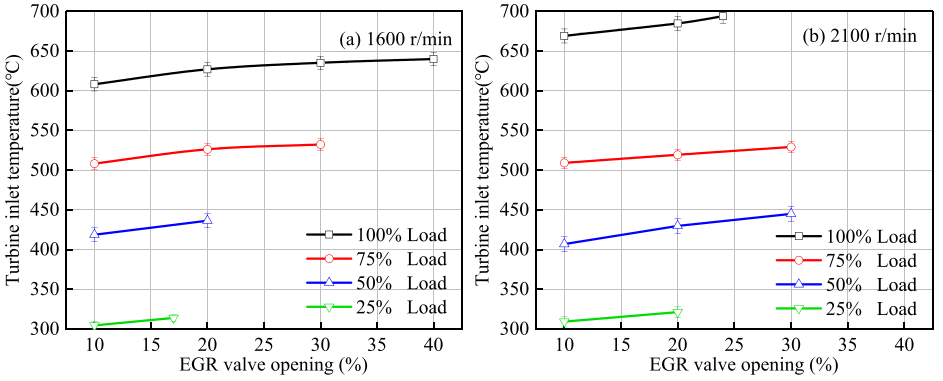

Figure 8. Effects of EGR valve opening on turbine inlet temperature under different loads: (a) 1600 r/min and (b) 2100 r/min.

https://doi.org/10.1021/acsomega.3c09052
ACS Omega 2024, 9, 8308−8319

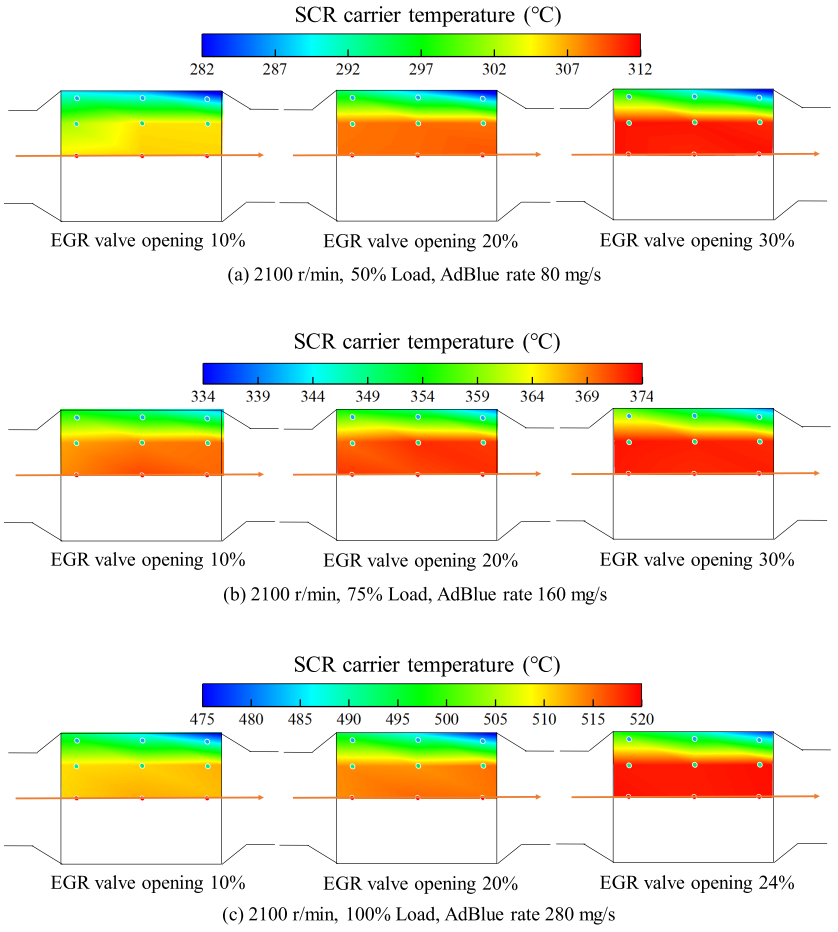

Figure 9. Effects of EGR valve opening on SCR carrier temperature under different loads at 2100 r/min.

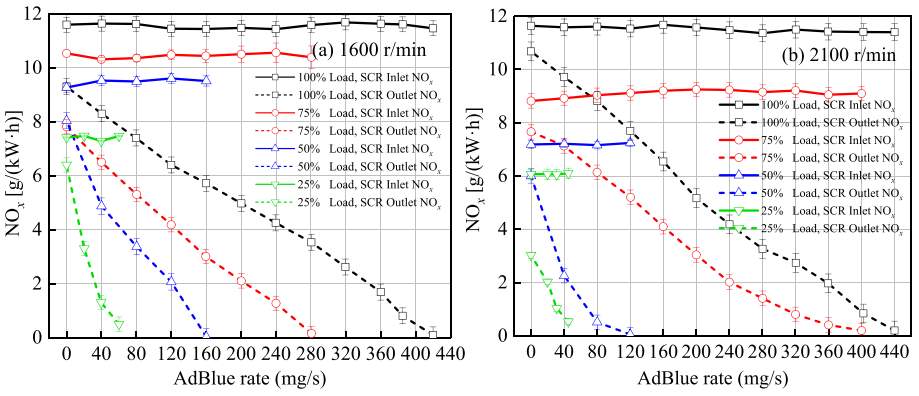

Figure 10. Effects of AdBlue rate on NO_x emission under different loads: (a) 1600 r/min and (b) 2100 r/min.

20, and 30%, respectively. The average temperatures of the cross section at the half radius of the axial direction were 368.6, 371.2, and 372.8 °C, respectively. The average temperatures of the edge cross section were 347.4, 347.1, and 348.2 °C, respectively. When the EGR valve opening was 10, 20, and 24% at 100% load of 2100 r/min, the mean cross section temperatures of the SCR carrier center were 511.4, 514.6, and 519.1 °C, respectively. The average temperatures of the cross section at a half radius of the axial direction were 510.9, 514.2, and 519.1 °C, respectively. The average temperatures of the edge cross section were 483.8, 484.7, and 488.3 °C, respectively.

3.2. Effects of AdBlue Rate. *3.2.1. Effects of AdBlue Rate on NO_x Emission and NO_x Conversion Efficiency.* Figure 10 shows the impacts of the AdBlue rate on the NO_x emissions at the SCR inlet and outlet under different loads at 1600 and 2100 r/min. With the increase of AdBlue rate, NO_x at the SCR outlet decreases, which was due to the ejection hydrolysis of urea into NH_3, and the conversion reaction of NH_3 with NO_x, which eventually leads to N_2 and H_2O. As the engine load increased, the NO_x emissions increased and more and more urea was needed. At 1600 rpm, the SCR outlet NO_x emission to the lowest value was close to zero and the AdBlue rates were 60, 160, 280, and 420 mg/s at 25, 50, 75, and 100% load, respectively. At 2100 r/min, the SCR outlet NO_x emission to

https://doi.org/10.1021/acsomega.3c09052
ACS Omega 2024, 9, 8308−8319

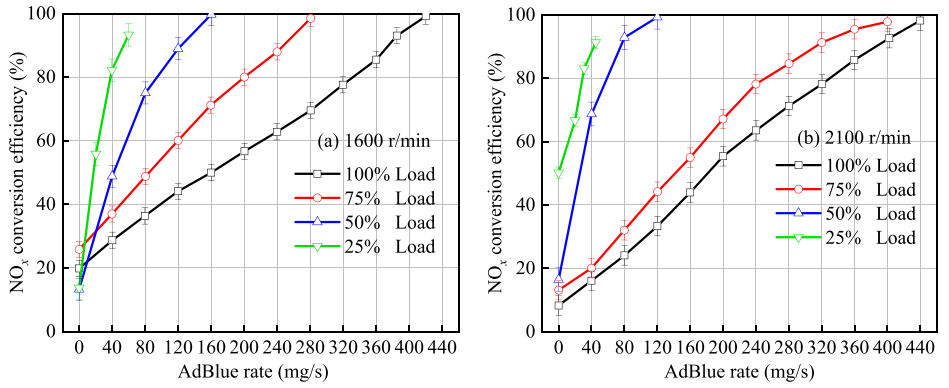

Figure 11. Effects of AdBlue rate on NO_x conversion efficiency under different loads: (a) 1600 r/min and (b) 2100 r/min.

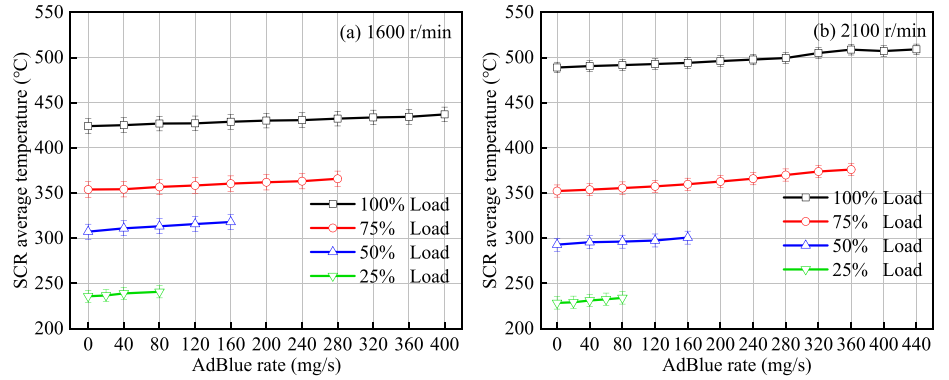

Figure 12. Effects of AdBlue rate on SCR average temperature under different loads: (a) 1600 r/min and (b) 2100 r/min.

the lowest value was close to zero and the AdBlue rates were 45, 120, 400, and 440 mg/s at 25, 50, 75, and 100% load, respectively.

Figure 11 shows the impacts of the AdBlue rate on the NO_x conversion efficiency under different loads at 1600 and 2100 r/min. With the increase of AdBlue rate, the NO_x conversion efficiency increased. At 1600 r/min, the highest NO_x conversion efficiencies were 93.3, 99.7, 98.4, and 99.1% at 25, 50, 75, and 100% loads. At 2100 r/min, the highest NO_x conversion efficiencies were 91.2, 99.2, 97.8, and 98.2% at 25, 50, 75, and 100% loads.

It can be seen from the data that the NO_x conversion efficiency was low at 25% loads, because the emission temperature of 25% load was low and the activity of SCR catalyst was insufficient, so the NO_x conversion efficiency was low.

3.2.2. Effects of AdBlue Rate on SCR Average Temperature. Figure 12 shows the impacts of the AdBlue rate on the SCR average temperature under different loads at 1600 and 2100 r/min. The SCR average temperature refers to the average value of nine temperature sensors inside the SCR carrier. As the AdBlue rate was increased, the SCR average temperature increased slightly. The SCR average temperature at different speeds was different especially under 100% load, the SCR temperature at 1600 r/min was about 425 °C, and the SCR temperature at 2100 r/min was about 550 °C. The reason for the increased of SCR average temperature was related to the chemical reaction inside the SCR carrier, with the increased of AdBlue rate, the more NO_x converted by SCR, and the more heat released.

3.2.3. Effects of AdBlue Rate on SCR Carrier Temperature. During the urea injection process, a chemical reaction occurred inside the SCR carrier. On the one hand, the urea injection reduced the temperature of the front end of the carrier. On the other hand, the reduction reaction between NH_3 and NO_x was an exothermic process. The internal reaction temperature of the support determines the activation energy of the catalyst, so the SCR temperature characteristics are the key to reduce NO_x emissions.

Figure 13 shows the impacts of the AdBlue rate on the SCR carrier temperature under 50, 75, and 100% load at 2100 r/min. As shown in the figure, the SCR carrier temperature was high in the middle and low at the edge, which was caused by the fact that the central airflow moves faster than the edge. In addition, the front temperature of the SCR carrier was low and the back temperature was high. This was because urea was injected at the front of the SCR, and urea absorbs the heat in the exhaust gas, resulting in a lower front temperature than the back end.

At 2100 r/min and 50% load, when the AdBlue rates were 20, 40, and 80 mg/s, the temperatures of the cross center section of the SCR carrier were 236.4, 238.4, and 241.4 °C, respectively. At 2100 r/min, 75% load, when the AdBlue rates were 80, 160, and 240 mg/s, the average temperatures of the cross center section of the SCR carrier were 365.8, 369.9, and 376.2 °C, respectively. At 2100 r/min and 100% load, when the AdBlue rates were 200, 280, and 360 mg/s, the average temperatures of the cross center section of the SCR carrier were 508.1, 511.4, and 518.9 °C, respectively.

3.3. Effects of EGR and AdBlue. *3.3.1. Effects of EGR and AdBlue on BSFC and NO_x.* Figure 14 shows the effects of EGR and AdBlue rate on BSFC and NO_x emissions under different loads at 1600 and 2100 r/min, respectively. With the increase of the AdBlue rate, NO_x emissions gradually decreased

https://doi.org/10.1021/acsomega.3c09052
ACS Omega 2024, 9, 8308−8319

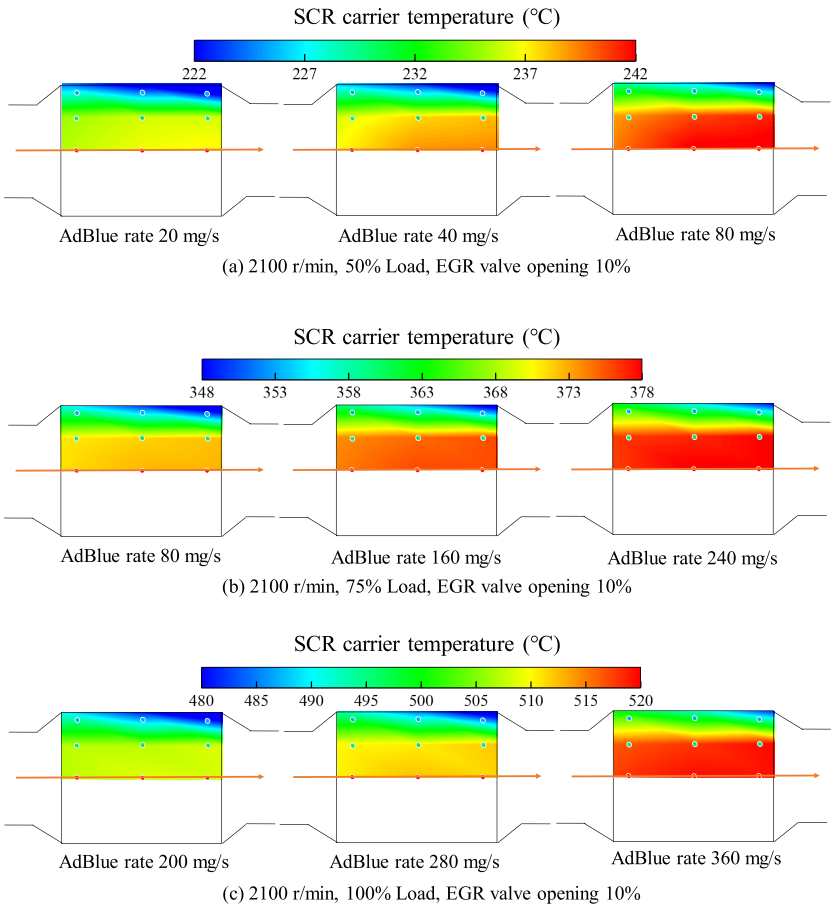

Figure 13. Effects of AdBlue rate on the SCR carrier temperature under different loads at 2100 r/min.

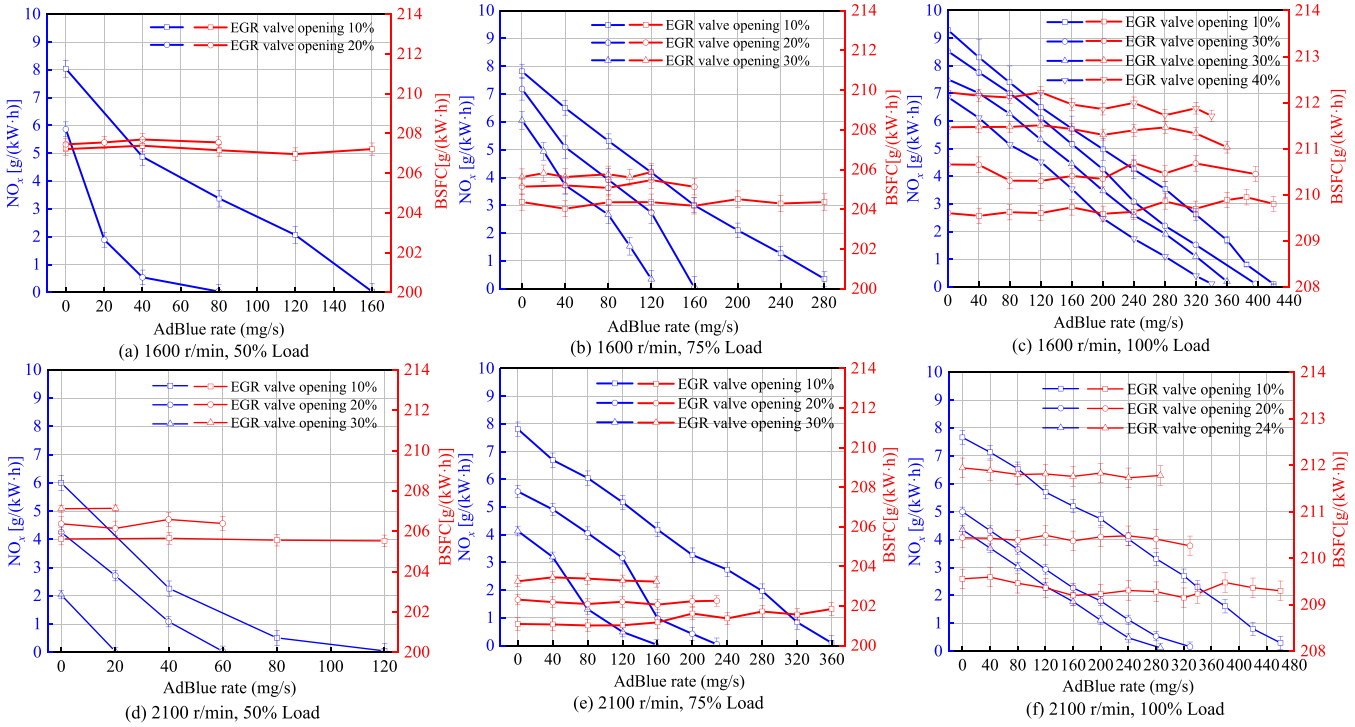

Figure 14. Effects of EGR valve opening and AdBlue rate on BSFC and NO_x under different loads at 1600 and 2100 rpm. (a) 1600 rpm, 50% load. (b)1600 rpm, 75% load. (c)1600 rpm, 100% load. (d) 2100 rpm, 50% load. (e) 2100 rpm, 75% load. (f) 2100 rpm, 100% load.

https://doi.org/10.1021/acsomega.3c09052
ACS Omega 2024, 9, 8308−8319

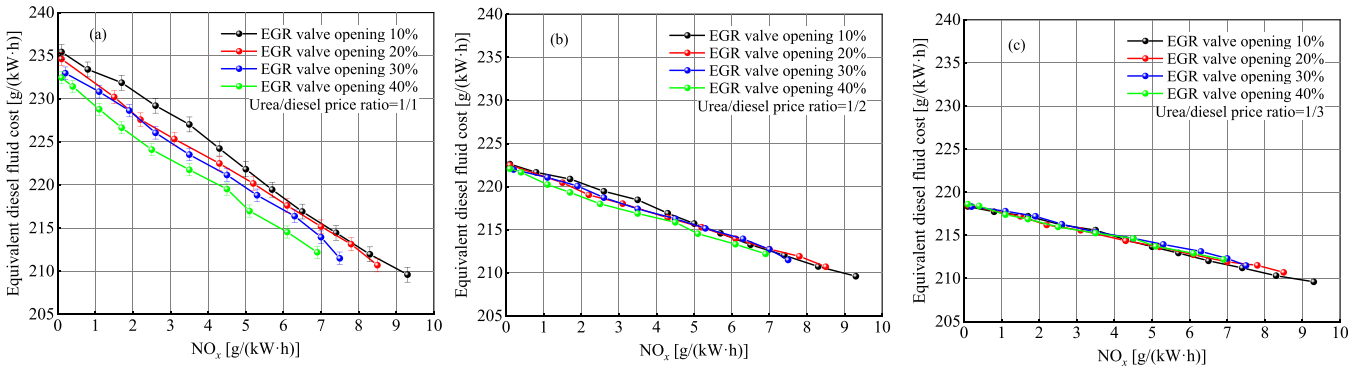

Figure 15. Comparison of total fluid costs. (a) Equivalent diesel liquid cost when the urea/diesel ratio was 1/1. (b) Equivalent diesel liquid cost when the urea/diesel ratio was 1/2. (c) Equivalent diesel liquid cost when the urea/diesel ratio was 1/3.

Table 4. Comparison of Total Fluid Costs

		total fluid costs		
	NO_x (g/kW·h)	urea/diesel price ratio = 1/1 (g/kW·h)	urea/diesel price ratio = 1/2 (g/kW·h)	urea/diesel price ratio = 1/3 (g/kW·h)
EGR valve opening 10%	0.1	235.4	222.6	218.3
	0.8	233.4	221.7	217.7
	1.7	231.9	220.9	217.2
	2.6	229.2	219.5	216.2
	3.5	227	218.5	215.6
	4.3	224.2	216.9	214.5
	5	221.8	215.7	213.7
	5.7	219.5	214.6	213
	6.5	216.9	213.3	212
	7.4	214.5	212	211.2
	8.3	212	210.7	210.3
	9.3	209.6	209.6	209.6
EGR valve opening 20%	0.1	234.6	222.5	218.5
	1.5	230.2	220.5	217.2
	2.2	227.6	219	216.2
	3.1	225.3	218	215.6
	4.3	222.5	216.4	214.4
	5.2	220.2	215.3	213.7
	6.1	217.6	214	212.7
	7	215.2	212.7	211.9
	7.8	213.1	211.9	211.5
	8.5	210.7	210.7	210.7
EGR valve opening 30%	0.2	233	222	218.3
	1.1	230.8	221.1	217.8
	1.9	228.6	220.1	217.2
	2.6	226.1	218.7	216.3
	3.5	223.5	217.4	215.4
	4.5	221.2	216.4	214.7
	5.3	218.8	215.4	213.9
	6.3	216.4	213.9	213.1
	7	213.9	212.7	212.3
	7.5	211.5	211.5	211.5
EGR valve opening 40%	0.1	232.4	222.1	218.6
	0.4	231.4	221.7	217.9
	1.1	228.8	220.2	217.2
	1.7	226.6	219.3	216.9
	2.5	224.1	218	216
	3.5	221.8	217.3	215.3
	4.5	219.5	215.9	214.6
	5.1	217	214.5	213.7
	6.1	214.5	213.3	212.9
	6.9	212.2	212.2	212.2

https://doi.org/10.1021/acsomega.3c09052
ACS Omega 2024, 9, 8308−8319

but the fuel consumption did not change. Different EGR valve openings have different effects on BSFC and NO_x emissions. From the results, increasing the EGR opening can reduce part of the NO_x emissions, which can reduce the consumption of AdBlue.

As shown in Figure 14a, in order to achieve the final zero NO_x emission, the AdBlue rate required 160 and 80 mg/s, respectively, at 10 and 20% of EGR valve openings. As shown in Figure 14b, in order to achieve the final zero NO_x emission, the AdBlue rate required 280, 160, and 120 mg/s, respectively, at 10, 20, and 30% of EGR valve openings. As shown in Figure 14c, in order to achieve the final zero NO_x emission, the AdBlue rate required 420, 400, 360, and 340 mg/s, respectively, at 10, 20, 30, and 40% of EGR valve openings. As shown in Figure 14d, in order to achieve the final zero NO_x emission, the AdBlue rate required 120, 60, and 20 mg/s, respectively, at 10, 20, and 30% of EGR valve openings. As shown in Figure 14e, in order to achieve the final zero NO_x emission, the AdBlue rate required 360, 225, and 160 mg/s, respectively, at 10, 20, and 30% of EGR valve openings. As shown in Figure 14f, in order to achieve the final zero NO_x emission, the AdBlue rate required 460, 325, and 280 mg/s, respectively, at 10, 20, and 30% of EGR valve opening, respectively.

3.3.2. Effects of EGR and AdBlue on Total Cost. EGR and SCR were the main technologies to reduce NO_x emissions. EGR reduces the original emissions of the engine but at the same time increases the consumption of diesel, resulting in poor economic performance of the engine. SCR needs to consume AdBlue. The total fluid cost of the diesel engine includes diesel and AdBlue. How to balance the overall economy of the engine is particularly important. Figure 15 and Table 4 show the comparison of total fluid costs at 1600 r/min (100% load, 350N·m). AdBlue was converted into equivalent diesel consumption for calculation. Figure 15a, b, and c show the results of the AdBlue/diesel price ratio according to 1/1, 1/2, and 1/3, respectively. As shown in the figure, as NO_x emissions decreased, the equivalent diesel fluid cost increased. According to the price ratio of AdBlue/diesel, 1/1, the maximum fluid cost was 235 g/(kW·h); according to the price ratio of 1/2 AdBlue−diesel, the maximum fluid cost was 223 g/(kW·h), and according to the price ratio of 1/3 urea diesel, the maximum fluid cost was 218 g/(kW·h). With the decrease of the AdBlue/diesel price ratio, EGR has less and less influence on fluid cost. Under the condition of zero NO_x, with the increase of EGR opening by 10%, the fluid cost decreases by 0.4, 0.07, and 0.04% respectively.

4. CONCLUSIONS

In the study, it was observed that as the EGR valve opening increased, several parameters of the engine underwent changes. Specifically, the air−fuel ratio and excess air coefficient decreased, leading to an increase in brake-specific fuel consumption (BSFC). Simultaneously, there was a decrease in NO_x emissions but an increase in exhaust temperature and SCR carrier temperature. Furthermore, with increasing engine loads, the air−fuel ratio and excess air coefficient decreased further, resulting in higher NO_x emissions, exhaust temperature, and SCR carrier temperature. However, it was found that the BSFC was at its lowest at 75% load, followed by 50 and 25% load.

Another aspect that was investigated in this research was the impact of AdBlue rate on NO_x emissions at the SCR outlet. It was observed that as the AdBlue rate increased, there was a decrease in NO_x emissions. However, with increasing engine load, the NO_x emissions also increased, requiring more urea to be injected. At an engine speed of 1600 r/min, the SCR outlet NO_x emission approached zero at the lowest value, with AdBlue rates of 60, 160, 280, and 420 mg/s at 25, 50, 75, and 100% load, respectively. Similarly, at 2100 r/min, the SCR outlet NO_x emission reached its lowest value close to zero, with AdBlue rates of 45, 120, 400, and 440 mg/s at 25, 50, 75, and 100% load, respectively. Additionally, as the AdBlue rate increased, there was a slight increase in the average SCR temperature. The temperature distribution on the SCR carrier indicated that the central section of the exhaust had a higher temperature compared to the edges, while the front temperature of the SCR carrier was lower than the back.

The study evaluated the effectiveness of EGR and SCR in reducing NO_x emissions from diesel engines. It was found that while EGR reduced NO_x emissions, it also had an impact on engine fuel consumption. On the other hand, SCR required the use of urea, which incurred costs. Both fuel consumption and urea consumption were considered as important factors in engine development. Interestingly, as NO_x emissions decreased, the equivalent diesel fluid cost increased. At 1600 r/min (100% load) when NO_x emissions were reduced to zero, the maximum fluid cost was determined to be 235, 223, and 218 g/(kW·h), for AdBlue/diesel price ratios of 1/1, 1/2, and 1/3, respectively. Furthermore, with a decrease in the AdBlue/diesel price ratio, the influence of EGR on fluid cost diminished. Under the condition of zero NO_x emissions, a 10% increase in EGR opening resulted in fluid cost reductions of 0.4, 0.07, and 0.04% for the respective AdBlue/Diesel price ratios mentioned above.

AUTHOR INFORMATION

Corresponding Author

Xuexuan Nie − *Yunnan Key Laboratory of Internal Combustion Engine, Kunming University of Science and Technology, Kunming 650500, China;* orcid.org/0000-0002-5031-2737; Email: 1838813119@qq.com

Authors

Size Zhang − *Yunnan Key Laboratory of Internal Combustion Engine, Kunming University of Science and Technology, Kunming 650500, China*

Yuhua Bi − *Yunnan Key Laboratory of Internal Combustion Engine, Kunming University of Science and Technology, Kunming 650500, China*

Jie Yan − *Yunnan Key Laboratory of Internal Combustion Engine, Kunming University of Science and Technology, Kunming 650500, China;* orcid.org/0000-0003-3479-3750

Shaohua Liu − *Yunnan Key Laboratory of Internal Combustion Engine, Kunming University of Science and Technology, Kunming 650500, China*

Yiyuan Peng − *Kunming Yunnei Power Co., Ltd., Kunming 650500, China*

Complete contact information is available at:

https://doi.org/10.1021/acsomega.3c09052
ACS Omega 2024, 9, 8308−8319

https://pubs.acs.org/10.1021/acsomega.3c09052

Notes

The authors declare no competing financial interest.

■ ACKNOWLEDGMENTS

This work was supported by the National Natural Science Foundation of China (project code 52066008) and the Major Science and Technology Special Program of Yunnan Provincial Science and Technology Department (Project code 202102AB080007). Guizhou Province Youth Science and Technology Talent Growth Project (Project code: Qianjiaohe KY Zi [2022] No. 111).

■ REFERENCES

(1) Shijin, SHUAI; Zhi, WANG; Xiao, M. A.; et al. Low carbon and zero carbon technology paths and key technologies of ICEs under the background of carbon neutrality[J]. *J. Automotive Safety and Energy* **2021**, *12* (04), 417−439. (in Chinese)

(2) Basaran, H. U.; Ozsoysal, O. A. Effects of application of variable valve timing on the exhaust gas temperature improvement in a low-loaded diesel engine[J]. *Applied Thermal Engineering* **2017**, *122*, 758−767.

(3) Li, H.; Song, C.; Lv, G.; et al. Assessment of the impact of post-injection on exhaust pollutants emitted from a diesel engine fueled with biodiesel[J]. *Renewable Energy* **2017**, *114*, 924−933.

(4) Reis, H.; Reis, C.; Sharip, A.; et al. Diesel exhaust exposure, its multi-system effects, and the effect of new technology diesel exhaust[J]. *Environ. Int.* **2018**, *114*, 252−265.

(5) Kagawa, J. Health effects of diesel exhaust emissions—a mixture of air pollutants of worldwide concern[J]. *Toxicology* **2002**, *181*, 349−353.

(6) Quiros, D. C.; Smith, J.; Thiruvengadam, A.; et al. Greenhouse gas emissions from heavy-duty natural gas, hybrid, and conventional diesel on-road trucks during freight transport[J]. *Atmos. Environ.* **2017**, *168*, 36−45.

(7) Jung, Y.; Pyo, Y.; Jang, J.; et al. Nitrous oxide in diesel aftertreatment systems including DOC, DPF and urea-SCR[J]. *Fuel* **2022**, *310*, No. 122453.

(8) Wang, D.; Cao, J.; Tan, P.; et al. Full course evolution characteristics of DPF active regeneration under different inlet HC concentrations[J]. *Fuel* **2022**, *310*, No. 122452.

(9) Kim, H. J.; Jo, S.; Kwon, S.; et al. NO_x emission analysis according to after-treatment devices (SCR, LNT+ SCR, SDPF), and control strategies in Euro-6 light-duty diesel vehicles[J]. *Fuel* **2022**, *310*, No. 122297.

(10) Zhao, Q.; Li, J.; Jiao, A.; et al. Pollutant emission characteristics of the close-coupled selective catalytic reduction system for diesel engines under low exhaust temperature conditions[J]. *Fuel* **2023**, *354*, No. 129303.

(11) Moon, S.; Park, S.; Son, J.; et al. Simplified Modeling and Analysis of Surface Temperature Distribution in Electrically Heated Catalyst for Diesel Urea-SCR Systems[J]. *Energies* **2022**, *15* (17), 6406.

(12) Liu, Y.; Tan, J. Experimental study on solid SCR technology to reduce NO_x emissions from diesel engines[J]. *IEEE Access* **2020**, *8*, 151106−151115.

(13) Guan, B.; Zhan, R.; Lin, H.; et al. Review of state of the art technologies of selective catalytic reduction of NO_x from diesel engine exhaust[J]. *Applied Thermal Engineering* **2014**, *66* (1−2), 395−414.

(14) Shuai, S.; Tang, T.; Zhao, Y.; Hua, L. State of the art and outlook of diesel emission regulations and aftertreatment technologies[J]. *J. Automotive Saf. Energy* **2012**, *3* (3), 200−17. (in Chinese)

(15) Praveena, V.; Martin, M. L. J. A review on various after treatment techniques to reduce NO_x emissions in a CI engine[J]. *Journal of the Energy Institute* **2018**, *91* (5), 704−720.

(16) Wang, J.; Shen, L.; Bi, Y.; et al. Modeling and optimization of a light-duty diesel engine at high altitude with a support vector machine and a genetic algorithm[J]. *Fuel* **2021**, *285*, No. 119137.

(17) Park, J.; Song, S.; Lee, K. S. Numerical investigation of a dual-loop EGR split strategy using a split index and multi-objective Pareto optimization. *Appl. Energy* **2015**, *142*, 21−32.

(18) Shiyu, L.; Boyuan, W.; Zexian, G.; et al. Experimental investigation of urea injection strategy for close-coupled SCR aftertreatment system to meet ultra-low NO_x emission regulation[J]. *Applied Thermal Engineering* **2022**, *205*, No. 117994.

(19) Zhang, Y.; Xia, C.; Liu, D.; et al. Experimental investigation of the high-pressure SCR reactor impact on a marine two-stroke diesel engine[J]. *Fuel* **2023**, *335*, No. 127064.

(20) Nie, X.; Bi, Y.; Liu, S.; et al. Impacts of different exhaust thermal management methods on diesel engine and SCR performance at different altitude levels[J]. *Fuel* **2022**, *324*, No. 124747.

(21) Lou, D.; Kang, L.; Zhang, Y.; et al. Effect of Exhaust Gas Recirculation Combined with Selective Catalytic Reduction on NO_x Emission Characteristics and Their Matching Optimization of a Heavy-Duty Diesel Engine[J]. *ACS omega* **2022**, *7* (26), 22291−22302.

(22) Ju, K.; Kim, J.; Park, J. Numerical prediction of the performance and emission of downsized two-cylinder diesel engine for range extender considering high boosting, heavy exhaust gas recirculation, and advanced injection timing[J]. *Fuel* **2021**, *302*, No. 121216.

(23) Mohiuddin, K.; Kwon, H.; Choi, M.; et al. Effect of engine compression ratio, injection timing, and exhaust gas recirculation on gaseous and particle number emissions in a light-duty diesel engine[J]. *Fuel* **2021**, *294*, No. 120547.

(24) Kumar, P.; Parwani, A. K.; Rashidi, M. M. Mitigation of NO_x and CO_2 from diesel engine with EGR and carbon capture unit[J]. *J. Therm. Anal. Calorim.* **2022**, *147* (16), 8791−8802.

(25) Kumar, M. V.; Babu, A. V.; Reddy, C. R.; et al. Investigation of the combustion of exhaust gas recirculation in diesel engines with a particulate filter and selective catalytic reactor technologies for environmental gas reduction[J]. *Case Studies in Thermal Engineering* **2022**, *40*, No. 102557.

(26) Cheng, W.; Li, X.; Yi, X. Influence of exhaust gas recirculation on low-load diesel engine performance[J]. *Wuhan University Journal of Natural Sciences* **2017**, *22* (5), 443−448.

(27) Zhang, X.; Sun, W.; Guo, L.; et al. Effects of Intake Components and Stratification on the Particle and Gaseous Emissions of a Diesel Engine[J]. *ACS omega* **2022**, *7* (12), 10001−10011.

(28) Mehregan, M.; Moghiman, M. Experimental investigation of urea injection parameters influence on NO_x emissions from blended biodiesel-fueled diesel engines[J]. *Environmental Science and Pollution Research* **2018**, *25*, 4303−4308.

(29) Diao, C.; Guo, X.; Li, J. Research on urea jet pump performance characteristics using the optimized NO_x removal equipment in diesel engine[J]. *Aerosol and Air Quality Research* **2018**, *18* (7), 1886−1990.

(30) Tan, P.; Li, X.; Wang, S.; et al. Selective catalytic reduction failure of low NH_3- NO_x ratio[J]. *Chinese Journal of Chemical Engineering* **2021**, *32*, 231−240.

(31) Qiu, T.; Song, X.; Lei, Y.; et al. Outlet temperature characteristics for NO_x catalyst container of diesel engine SCR system and its calculation model[J]. *Trans. CSAE* **2016**, *32* (6), 89−94. (in Chinese)

(32) Schönebaum, S.; Dornseiffer, J.; Mauermann, P.; et al. Composition/performance evaluation of lean NO_x trap catalysts for coupling with SCR technology[J]. *ChemCatChem.* **2021**, *13* (7), 1787−1805.